Molecular-dynamics simulation of two-dimensional thermophoresis

Ricardo Paredes V.,[1] Vladimir Idler,[2] Anwar Hasmy,[1] Victoria Castells,[1] and Robert Botet[3]
[1]*Laboratorio de Física Estadística de Sistemas Desordenados, Centro de Física, IVIC, Apartado 21827, Caracas 1020A, Venezuela*
[2]*Departamento de Física, Facultad de Ciencias y Tecnología, Universidad de Carabobo, Apartado 129, Código Postal 2001, Casilla 12, Valencia, Venezuela*
[3]*Laboratoire de Physique des Solides, CNRS UMR No. 8502 Bâitment 510, Centre d'Orsay, Université Paris-Sud, Orsay 91405, France*
(Received 22 February 2000)

A numerical technique is presented for the thermal force exerted on a solid particle by a gaseous medium between two flat plates at different temperatures, in the free molecular or transition flow. This is a two-dimensional molecular-dynamics simulation of hard disks in a inhomogeneous thermal environment. All steady-state features exhibited by the compressible hard-disk gas are shown to be consistent with the expected behaviors. Moreover the thermal force experienced by a large solid disk is investigated, and compared to the analytical case of cylinders moving perpendicularly to the constant temperature gradient for an infinite Knudsen number and in an infinite medium. We show precise examples of how this technique can be used simply to investigate more difficult practical problems, in particluar the influence of nonlinear gradients for large applied differences of temperature, of proximity of the walls, and of smaller Knudsen numbers.

PACS number(s): 51.10.+y, 65.70.+y, 51.30.+i, 05.10.−a

I. INTRODUCTION

Over a century ago, Tyndall [1] observed that dust particles suspended in a gas with inhomogeneous temperature tend to move out of the hot regions. This constitutes the pioneering experimental study of thermophoresis in a gas. Because of its large magnitude in rarefied medium, the appearance of such a diffusion current in the gaseous fluid is of major importance in aerosol science as well as aerosol industry. As a simple example, thermal precipitators are commonly used to clean up dusty gas [2], and quantitative comprehension of this phenomenon is essential in designing practical devices in which the behavior of such particles is well controlled. Potential or existing applications for stability, movement and deposition of small particles in the inhomogeneous medium are indeed numerous in various areas of physics, engineering, and biology.

This particle migration is the result of a force (the thermal force) experienced by the dust particle in a temperature gradient. In a first approximation (of small spatial temperature variations) this thermal force should be just proportional to this gradient. Moreover, in an infinite dispersing medium, this force is expected to depend essentially on two nondimensional parameters: Kn, the Knudsen number related to the particle: (the ratio of the molecular mean-free path λ, and the typical length size of the particle), and the ratio Λ of the thermal conductivities of the particle k_p and the gas k_g. Note that the Knudsen number related to the whole finite system (as the ratio of λ and the typical size of the system) should play a role [3], but it is usually not taken into account for simplicity.

Since the unit of force on the particle of surface S is just PS, with P the pressure of the gas (which is assumed to be homogeneous throughout the system), the thermal force F_{th} is assumed to have the form

$$\mathbf{F}_{th} = A(\mathrm{Kn},\Lambda) PS \frac{\lambda \nabla T}{T}, \tag{1}$$

where ∇T is the gas temperature gradient ''felt'' by the particle, and T is the average temperature of the particle. The nondimensional parameter $A(\mathrm{Kn},\Lambda)$ should also depend on the shape of the particle. The calculation of this parameter, even for such a simple geometry as that of a sphere, is far from being complete for all values of Kn and Λ [4]. The free molecular flow (i.e., the extreme rarefied gas $\mathrm{Kn}\sim\infty$), was well studied for spheres [5] and cylinders [6]. In effect, in this case, one can make the approximation that the particle is so small as compared to the molecular mean free path that it does not affect the velocity distribution of the molecules hitting the particle. The analytical problem is then split into two steps: first the velocity distribution of the gas molecules is calculated, then this distribution in the momentum transfer-calculation method is applied on the particle. The influence of the distance x to the hot wall was also investigated by Williams [7], and the constant $A(\mathrm{Kn},\Lambda,x/\lambda)$ seen indeed to depend (slightly) on the distance to the wall. These results for an infinite Knudsen number were extended [8] to large but finite values of Kn, calculating the first order perturbation (in 1/Kn) of the linearized BGK model [9], used here as a correct approximation of the full steady-state Boltzmann equation. In this way, closed analytical expressions were derived. This is no longer the case for the transition regime ($\mathrm{Kn}\sim 1$), where only numerical calculations of the solutions of the linearized BGK model are available [10]. In the present work we shall not discuss the other possible limit $\mathrm{Kn}\sim 0$, which was investigated analytically with different tools [11].

In this paper, we are interested in the case where the Knudsen number is essentially finite, but large. This corresponds to a rarefied gas with solid particles of typical size smaller than, or of the same order, as, the molecular mean free path. Instead of taking the viewpoint of the linearized (approximate of the) Boltzmann equation, we should like to pose the question of whether these results can also be obtained by means of a molecular-dynamics (MD) simulation

of the gas flow around the particle considered as an obstacle. There is presently a great deal of MD techniques incited by the constant and inescapable growth of computer capacities. Moreover, these techniques have proved to give quantitatively correct results even for a modest number of molecules (as compared to real experiments) [12]. In particular, MD simulations were applied to study flows over simple objects like flat planes and cylinders [13,14]. One can then imagine that such tools could be used to recover theoretical results on the thermophoresis of particles of simple shape in a gas, when the approximations used to derive the analytical solutions are valid. However, in such MD simulations, there is not an *a priori* limitation by the necessary smallness of the temperature gradient, the shape of the particle, or the value of the Knudsen number, as long as the local equilibrium can be reached. A detailed investigation of this approach in the simple case of two-dimensional simulations of compressible hard-disk fluid motion around a disk particle is the main objective of the present work, keeping in mind that the generalization to a more complex three-dimensionsal fluid around a fractal aggregate in the gravitational field (for example) is straightforward from the point of view of numerical implementation [15]. There are others simulation methods that can be used to study the thermophoresis effect. One of them is the direct simulation Monte Carlo method (see, for example, Ref. [16]). This method can be faster than MD, specially at low densities [17]; however, we chose MD because it can be generalized directly to any situation, as stated above, without any *ad hoc* approximation. In Sec. II, we give details about the model of hard disks, the boundary conditions and the rules of interactions during molecular collisions. In Sec. III, we describe the MD hard-disk simulations for a fluid enclosed in two plates at different temperatures (without any particle inside), and discuss the problems of the characteristic time required to reach local equilibrium, the temperature jumps at the walls, and the dependence of the temperature gradient obtained with the imposed difference of wall temperatures. In Sec. IV, a disk of various radius and infinite thermal conductivity is inserted in the fluid at a specific position, and we show how the particle reaches its final temperature, and the nature of the net thermal force acting on it. The dependence of this force with the Knudsen number, its radius, and its distance to the walls is discussed.

II. HARD-DISK MODEL

We consider a system of N hard disks (molecules) of diameter $\tilde{d}_g=1$ and mass $\tilde{m}_g=1$ (the length unit and the mass unit in the system, respectively), allowed to move in a rectangular area of size $L_x \times L_y$. There is no external field, and the Boltzmann constant k_B is set equal to 1 in all our simulations. The boundary conditions are periodic in the ''vertical'' y direction ($y=0$ and $y=L_y$), while in the ''horizontal'' direction the system is limited by two thermal walls at the positions $x=0$ and $x=L_x$. These walls are maintained at constant temperatures of $T_{w,c}$ and $T_{w,h}$ (both temperatures may be similar), respectively, and can be considered as two perfect heat reservoirs. When a molecule hits a wall, it is thermalized in the sense that its velocity is sampled randomly accordingly to the probability density

$$\phi(v_x)=\frac{m}{k_B T_w} v_x \exp\left(-\frac{m v_x^2}{2 k_B T_w}\right) \tag{2}$$

for the x component [with $v_x \geqslant 0$ at the cold wall ($x=0$), and $v_x \leqslant 0$ at the hot wall ($x=L_x$)], and a Maxwellian distribution at the temperature of the wall,

$$\phi(v_y)=\sqrt{\frac{m}{2\pi k_B T_w}} \exp\left(-\frac{m v_y^2}{2 k_B T_w}\right), \tag{3}$$

for the y component of the velocity. This nonequilibrium ideal accomodation was demonstrated to lead to the correct Fourier's law [18,19], correct thermalization of the system [20], and correct temperature and density profiles near the thermal walls [21]. Inside the box, hard disks undergo elastic collisions between them.

Here we deal only with a calculation of the thermal force. The solid particle is maintained motionless in a fixed position, and the force is calculated when the gas has reached its steady state. This means that the particle diffusion coefficient is assumed to be much smaller than the gas kinematic viscosity. The collision between a molecule and the particule is submitted to the same rule as for the thermal wall [Eqs. (2) and (3)], with T_w now the temperature of the particle. But the particle is considered as finite (though much larger than the molecule) and its thermal conductivity infinite, so its temperature must change according to

$$\Delta T=\frac{\Delta E}{C_P}, \tag{4}$$

where ΔE is the opposite of the change in energy of the striking molecule, before and after the collision, and C_P is the heat capacity of the particle at a constant pressure. For a two-dimensional solid at ordinary temperatures, this heat capacity is of the order of magnitude or $2k_B$ per atom of solid. Since there are about $(2\tilde{R}/\tilde{d}_g)^2$ of such atoms in a disk of radius $\tilde{R}$, and the values of $\tilde{d}_g$ and k_B have been fixed conventionally to 1, one obtains C_P, proportional to $\tilde{R}^2$ with a multiplicative constant of order 1 in our units. We have then taken

$$C_P=\tilde{R}^2 \tag{5}$$

for the particle heat capacity in our simulations below. This completes the set of interaction rules (molecule-wall, molecule-molecule, and molecule-particle) used in the present two-dimensional MD simulations [22].

In principle, the time evolution can be studied as well, even if this is not the central problem of the present work. Our MD simulation runs just a sequence of collisional events (MD steps). To transform these steps into time information, we need to quote the relation between the time that we can compute with our units, and the physical time. To achieve this point, we need to define our system of four fundamental units (length, mass, time, and temperature) properly according to the choices $\tilde{d}_g=1$, $\tilde{m}_g=1$, and $k_B=1$, and to fix one temperature in the system; for instance, the cold wall is set at temperature: 10 (this is our choice for all the simulations presented here). Schematically (if needed, precise values for

the radius, mass of the gas molecules, and temperature should be used), during one step, a molecule with Boltzmann temperature $\tilde{T}$ moves on a distance $\tilde{l}$ at velocity $\tilde{v}$ all with our units of temperature, length, and time. These distance, velocity, and temperature are related to the physical ones (l, v, and T, respectively) through

$$\tilde{l} = l/d_g, \tag{6}$$

$$\tilde{v} = v/\sqrt{k_B T_{w,c}/10m_g}, \tag{7}$$

$$\tilde{T} = 10T/T_{w,c}, \tag{8}$$

with $T_{w,c}$ the real temperature of the cold wall in K, and d_g and m_g the real diameter and mass of one gas molecule. Note that the real temperature T must be in a reasonable range where radiative forces are negligible (this is indeed the general case for ordinary applications). This means that the time increment $\delta\tilde{t}$ computed by considering that $\tilde{l}/\tilde{v}$ is related to the physical time increment through

$$\delta t = c\,\delta\tilde{t} = d_g\sqrt{10m_g/k_B T_{w,c}}\,\delta\tilde{t}. \tag{9}$$

If one knows the values of d_g and m_g for real gas molecules, and the real temperature of the cold wall, the scaling coefficient c can be readily calculated. For argon at room temperatures ($d_g \simeq 3\times10^{-10}$ m and $m_g \simeq 6.710^{-26}$ kg), one finds that δt is a fraction of nanoseconds for the MD increment of time $\delta\tilde{t}=1$.

In our simulations, the typical system size was $\tilde{L}_x \sim 3800$ (the distance between walls) and $\tilde{L}_y \sim 5700$. We investigated gas densities from 0.0003 (6500 molecules) to 0.004 (87000 molecules). We ran simulations over times $\tilde{t}$ of order 10^6 ($t\sim0.1$ ms) for the lowest density case and over $\tilde{t}$ of order 10^4 ($t\sim1$ μs) for the highest density case. These are long times for systems whose typical lengths are several μm.

III. THERMAL STATIONARY STATE (HARD-DISK GAS)

We begin with a discussion of the appearance of the thermal gas stationary state in a system without any solid particle inside. At the beginning of each such simulation, the velocity of each molecule is taken from a Maxwell distribution at a temperature equal to an intermediate value, the most used being $(\tilde{T}_{w,h}+\tilde{T}_{w,c})/2$. Moreover, as explained previously, $\tilde{T}_{w,c}$ has been set equal to 10. In such a way we are allowed to fix one temperature in the system to an arbitrary positive value, since change: $T\rightarrow\alpha T$ in the entire system simply implies a rescaling of all the forces defined as change of momentum per unit of time: $F\rightarrow\alpha F$. A transient stage develops, reaching the steady state after some time. This is shown in Fig. 1 for the time evolution of the gas temperature near the two walls. After some short characteristic time (which is nothing but $L_x L_y/\lambda\overline{v}$, with $\overline{v}$ the average velocity of gas molecules), the gas temperature near the two walls fluctuates around definite values which are different from the wall temperatures. In this example, these values $\tilde{T}_c = 18$ instead of $\tilde{T}_{w,c}=10$, and $\tilde{T}_h = 46$ instead of $\tilde{T}_{w,h}=70$. The average temperature of the gas is $\tilde{T}_{avg}=31$. These temperature jumps, between the wall and adjacent fluid, are well known experimentally, and were discussed in detail for Lennard-Jones numerical simulations [19]. A plot of the temperature profile is shown in Fig. 2. It shows the difference between the imposed difference of the wall temperatures and the obtained gradient in three cases: the gradient in Fig. 2(a) is for a case of larger density ($\tilde{\rho}=0.004$), the same temperature difference between walls ($\Delta\tilde{T}=60$) as for the case shown in Fig. 2(b)

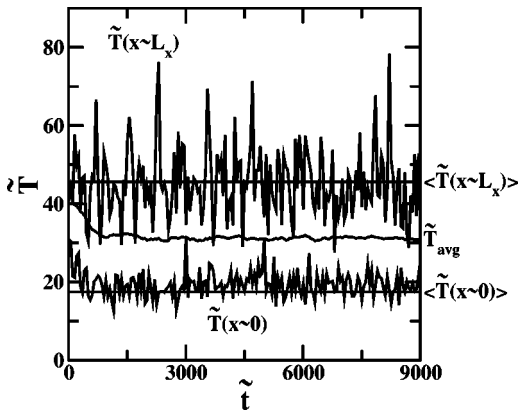

FIG. 1. Example of gas temperatures $\tilde{T}_h$ and $\tilde{T}_c$, respectively, near the hot wall ($x\sim L_x$) and near the cold wall ($x\sim0$) as a function of MD time for a system of density $\tilde{\rho}=0.0005$ corresponding to 10 800 particles in a box ($\tilde{L}_x=3800$, $\tilde{L}_y=5700$). The mean-free path of the gas molecules is $\tilde{\lambda}=1160$. The hot wall is maintained to a fixed temperature $\tilde{T}_{w,h}=70$, and the cold wall to a temperature $\tilde{T}_{w,c}=10$. Despite the fluctuations, the average values are clear (they are plotted as horizontal lines). The middle curve with small fluctuations is the average value of the gas temperature $\tilde{T}_{avg}=31$ throughout the system. Time averages shown in the figure were taken after the system reached steady state (typically $10^5<\tilde{t}<1.5\times10^6$).

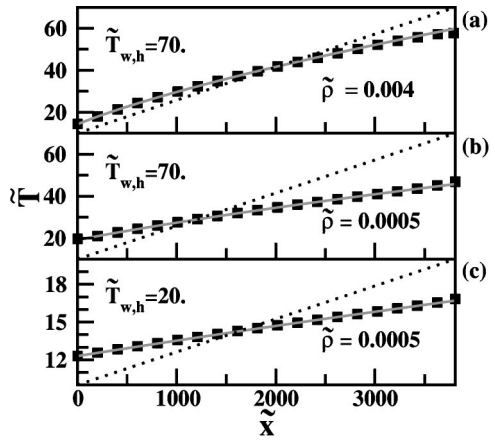

FIG. 2. Three examples of temperature profiles (squares). System size: ($\tilde{L}_x=3800$, $\tilde{L}_y=5700$). Thin lines are analytical fits, and dotted lines are linear functions if there is no temperature jumps. (a) The low-density case: $\tilde{\rho}=0.004$ and the temperatures of the cold and hot walls are $\tilde{T}_{w,c}=10$ and $\tilde{T}_{w,h}=70$, respectively. The gas mean free path is $\tilde{\lambda}=128$. (b) $\tilde{\rho}=0.0005$, $\tilde{\lambda}=1160$, $\tilde{T}_{w,c}=10$, and $\tilde{T}_{w,h}=70$. (c) $\tilde{\rho}=0.0005$, $\tilde{\lambda}=1160$, $\tilde{T}_{w,c}=10$, and $\tilde{T}_{w,h}=20$.

($\tilde{\rho}=0.0005$). The case shown in Fig. 2(c) has the same density and a smaller temperature difference between walls ($\Delta\tilde{T}=10$) then in Fig. 2(b). Finally, Fig. 2(c) shows a small gradient for which the linearized Boltzmann equation is expected to describe the thermodynamics of the system. For a larger gradient and density one notes a pronounced nonlinearity of the temperature profile: the temperature gradient is no longer constant throughout the system.

A simple argument leads to a good fit of this sort of profile: writing the Fourier law for the heat current as

$$\mathbf{J}_Q=-k_g\nabla T, \tag{10}$$

and supposing that $\nabla\mathbf{J}_Q$ is vanishing because the system has reached its steady state and the macroscopic gas velocities are supposed to be small, we obtain the equation

$$\nabla(k_g\nabla T)=\mathbf{0}. \tag{11}$$

The state-dependent gas thermal conductivity for a two-dimensional compressible gas of hard disks at density ρ and temperature T is [23]

$$k_g=k_o(\rho)\sqrt{T}, \tag{12}$$

with $k_o(\rho)$ a known function of the density, which remains about constant for small values of ρ. We deduce that the profile temperature must behave like

$$T(x)=[T_h^{3/2}x/L+T_c^{3/2}(1-x/L)]^{2/3}, \tag{13}$$

with T_h and T_c the gas temperature in the vicinities of the hot and cold walls, respectively. This is indeed a rough approximation, but here we do not need a better one [24], since it perfectly fits the results of the simulations, which give the correct result (apart from the fluctuations and possible bias very close to the hot wall). These fits are shown in Fig. 2 for comparison.

For practical applications, large temperature gradients are required to obtain the largest effects possible [25] (for example, to produce large thermophoresis). This problem can be accessed here naturally—unlike analytical approaches, which cannot be performed when linearization of the Boltzmann equation breaks down.

The relation between the temperature jumps at the walls and the imposed wall temperature differences is expected to be linear at least for small enough gradients [19]. This is shown in our numerical experiments in Fig. 3, and we see that, as is generally the case, the jump near the hot wall is larger than that near the cold one. But these linearity relations here seem to be only approximately verified, and deviations from linearity are clear for the large temperature differences. There is presently no available analytical investigation of this phenomenon when nonlinearities begin to occur.

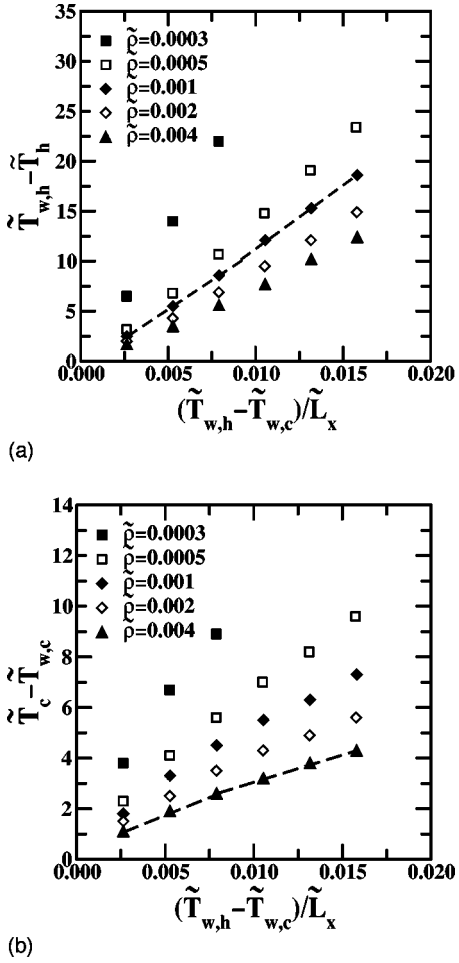

FIG. 3. (a) Temperature jump between the hot-wall temperature and the gas temperature close to it vs the real temperature gradient. Crossover between the low-gradient linear regime and the nonlinear high-gradient effect is seen here for gradients of order 10^{-2}. (b) Temperature jump between the gas temperature near the cold wall and the cold-wall temperature vs the real temperature gradient. Crossover between the low-gradient linear regime and the nonlinear high-gradient effect is seen for the same value of the gradients as in the (a).

IV. THERMAL FORCE ACTING ON THE PARTICLE

When a circular particle is placed inside the system, we have to check first that it reaches its final temperature within a reasonable time; that is to say, comparable to the relaxation time for the gas. This is shown in Fig. 4 where its temperature is plotted as a function of the physical time. Since the thermal conductivity of the particle here is supposed to be infinite, its temperature is indeed homogeneous. Figure 5 also shows the temperature pattern in the system.

In our simulation we can now compute the thermal force F_{th} acting on the particle as a result of the total momentum transfer from the gas molecules per unit of physical time. The time interval $\delta\tilde{t}$ is here equal to 5 for simulations going from 10 000 to 2 000 000, with the chosen units (corresponding to some nanoseconds compared to a total simulation of 1–100 μs). This is the same technique as for analytical derivations, but we dispose of the difficult task of obtaining the proper velocity distribution of the incoming particles, since this distribution is built by the numerical simulation itself.

In Fig. 6(a) we plot some examples of $\tilde{F}_{th}$ vs the temperature gradient $\nabla\tilde{T}$ for the same system geometry, same molecule density, and various radii of the particle. The temperature gradient has been estimated as the best linear fit in the particle region. The local (time-averaged) pressure was

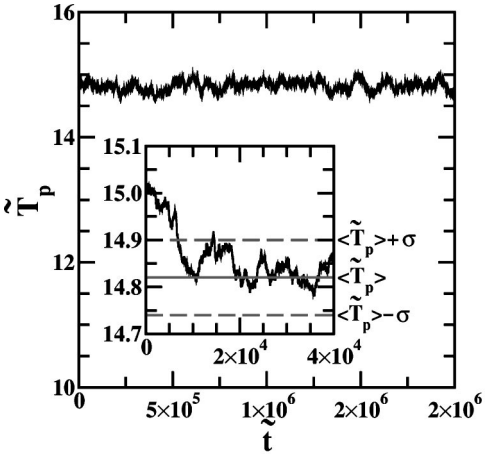

FIG. 4. Plot of the temporal evolution of the particle temperature. Inset: the very beginning of this evolution showing the fast thermalization of the temperature. σ is the standard deviation of the data. In this case, the system size is ($\tilde{L}_x=3800$, $\tilde{L}_y=5700$), the gas density is $\tilde{\rho}=0.0003$, and the temperatures of the hot and cold walls are $\tilde{T}_{w,c}=10$ and $\tilde{T}_{w,h}=20$.

checked to be approximately constant inside the whole system. Except for the largest radius used, formula (1) is then well recovered, with $S=2\pi R$ since the system is two-dimensional. The thermal force can be written in the form

$$\mathbf{F}_{th}=2\pi A(\mathrm{Kn},\infty)\lambda PR\frac{\nabla T}{T}, \tag{14}$$

with P/T almost constant (this is the average gas density), and $A(\mathrm{Kn},\infty)$ a constant. The linearity of F_{th} with the radius R is checked in Fig. 6(b). Not surprisingly, we find the same resulting R dependence as for three-dimensional cylinders perpendicular to the constant temperature gradient [6]

$$\mathbf{F}'_{th}=-\frac{3}{4}\sqrt{\pi}\lambda PR\frac{(\nabla T)_\infty}{T}, \tag{15}$$

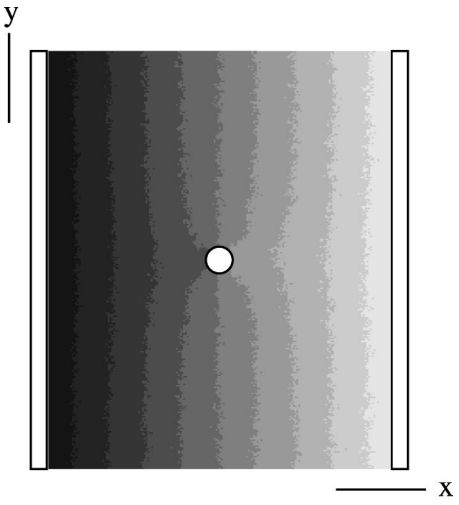

FIG. 5. Temperature pattern for a system with $\tilde{\rho}=0.0005$, $\tilde{R}=162$, $\tilde{T}_{w,c}=10$, and $\tilde{T}_{w,h}=20$. Darker colors mean lower temperatures. In the figure we also schematically show the particle and the cold (left) and hot (right) walls.

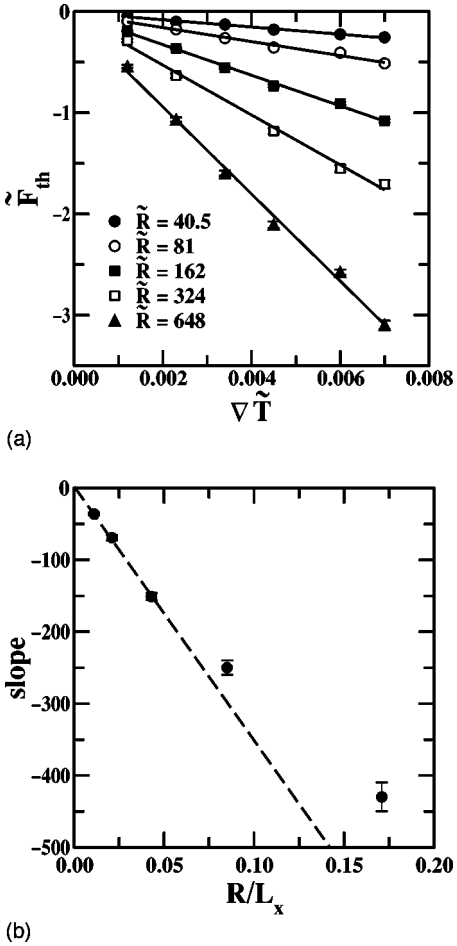

FIG. 6. (a) Plot of the thermophoretic force $\tilde{F}_{th}$ vs the temperature gradient $\nabla\tilde{T}$ for the same system geometry ($\tilde{L}_x=3800$, $\tilde{L}_y=5700$), the same gas density ($\tilde{\rho}=0.0005$), and various radii of the particle $\tilde{R}$. The temperature gradient has been estimated as the best linear fit in the particle region. Except for the largest radius used, the linear dependence of the force with radius is well recovered, as shown in (b).

where $(\nabla T)_\infty$ is the temperature gradient inside the system far from any (wall) boundary, and $\mathbf{F}'_{th}$ is the force per unit length of the cylinder. The average molecular mean free path λ is constant in all the data of the Fig. 6, as the average gas density.

The deviations seen in Fig. 6(b) from the expected law [Eq. (14)] are due to the finite size effects of the box, the ratio R/L characterizing these effects which become large enough (0.17 for the last point). Treatment of this problem is known to be one of the most important challenges in the context of applications when considering the design of thermal filters [3].

To analyze the problem in the vicinity of the walls in more detail, we performed numerical simulations with the particle of a given radius at different positions x_0 from the walls. The results are presented in Fig. 7. In Fig. 7(b), we see small deviations of the thermal forces due to the proximity of the walls. This effect was previously investigated analytically in the limit of the infinite Knudsen number [7].

Another point is that, when the nondimensional coefficient $A(\mathrm{Kn},\infty)$ does not vary (which is expected for very

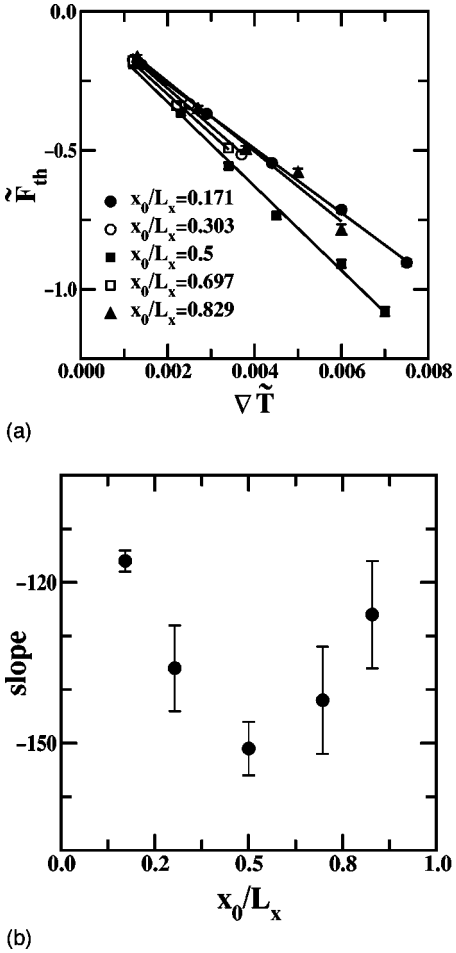

FIG. 7. (a) Plot of the thermophoretic force $\tilde{F}_{th}$ vs the temperature gradient $\nabla\tilde{T}$ for the same system geometry ($\tilde{L}_x=3800$, $\tilde{L}_y=5700$), the same particle radius ($\tilde{R}=162$), the same gas density ($\tilde{\rho}=0.0005$), and various locations of the particle inside the box. $\tilde{x}_0$ denotes the abscissa of the center of the particle. (b) The largest thermophoretic effect occurs when the particle is located at the center of the system.

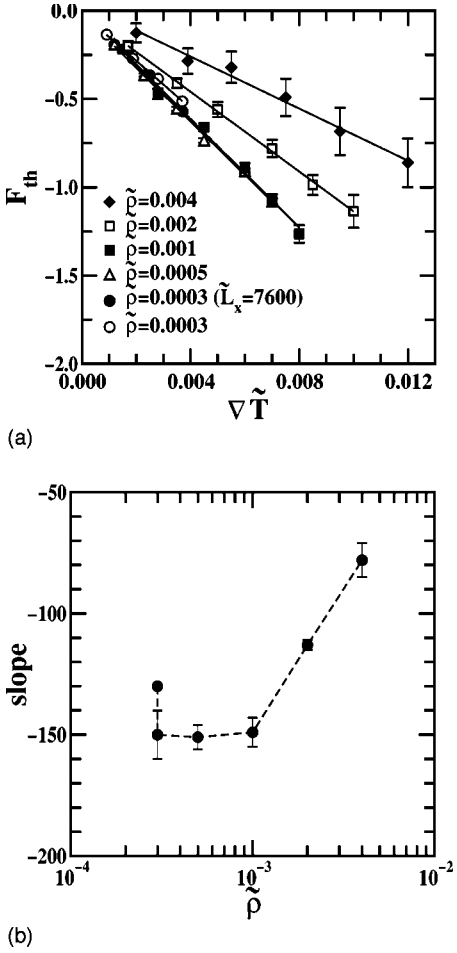

FIG. 8. (a) Plot of the thermophoretic force $\tilde{F}_{th}$ vs the temperature gradient $\nabla\tilde{T}$ for the same system geometry ($\tilde{L}_x=3800$, $\tilde{L}_y=5700$), the same particle radius ($\tilde{R}=162$), and various gas densities. The system for lowest density $\tilde{\rho}=0.0003$ has been investigated for two different system lengths to see the effect of the ratio λ/L_x on the thermophoretic force. $\tilde{L}_x=3800$, which is of same order as the gas mean free path ($\tilde{\lambda}=2620$), and $\tilde{L}_x=7600$. (b) As expected, the force is independent of ρ when the density is small, and the ratio λ/L_x large enough. When $\tilde{\rho}$ becomes larger than 10^{-3}, the thermophoretic force tends to decrease, as the system goes out of the free molecular flow regime.

large Knudsen numbers) formula (14) [or Eq. (15) as well] predicts the independence of the thermophoretic coefficient vs the gas density, since $\lambda P/T$ is on average independent of the gas density. This is shown in Fig. 8, in which deviations are seen [Fig. 8(b)] when the density is so large that coefficient $A(\mathrm{Kn},\infty)$ cannot be considered as a constant.

Finally, Eq. (15) can be written as $\tilde{\mathbf{F}}'_{th}=-\frac{3}{4}\sqrt{\pi}\tilde{\lambda}\tilde{\rho}\tilde{R}(\nabla\tilde{T})_\infty$. Using the corresponding average gas density ($\tilde{\rho}=0.0005$) and the mean free path, estimated from simulations at equilibrium ($\tilde{\lambda}=1160$), the coefficient $\frac{3}{4}\sqrt{\pi}\tilde{\lambda}\tilde{\rho}$ obtained is about 18% below the slope of the straight line in Fig. 6(b). On the other hand, using $\tilde{\lambda}\tilde{\rho}\sim 0.6$, from simulations at equilibrium, and the corresponding particle radius ($\tilde{R}=162$), the coefficient $\frac{3}{4}\sqrt{\pi}\tilde{\lambda}\tilde{\rho}\tilde{R}$ is 15% below that the constant value obtained in the low density limit in our simulations of the thermophoresis effect [Fig. 8(b)]. In both cases, agreement is excellent, in spite of simulations being performed for two-dimensional systems, and that we are comparing with a similar three-dimensional case.

V. SUMMARY AND CONCLUSIONS

In this work we have presented molecular dynamics simulations of system of hard disks in a nonequilibrium thermal environment. Though simple, they capture the main features expected in such a system: temperature jumps at interfaces with heat reservoirs, and stable temperature profiles. This complements previous quantitative agreement found in hydrodynamics (analytical and numerical) analysis of the compressible hard-disk fluid [26]. Thermal effects on a particle of infinite heat conductivity, placed anywhere between the two plates, has been studied. However, on a higher level, we have seen how this technique could be useful to investigate problems which are quite difficult to handle analytically: nonlinear effects for high enough temperature differences have been reported, as well as the effects of proximity of the wall for various Knudsen numbers. This shows the power of

the method. Even if analytical results (or numerical results on analytical solutions) are necessary to obtain a precise understanding of the problem of thermophoresis, these MD simulations provide a complementary alternative to study unexplored areas, in particular thermal forces on particles of non-simple shapes, which is in fact very interesting for the industry and not possible to deal with analytically.

ACKNOWLEDGMENTS

CNRS-CONICIT Nos. 5789 and 7195, exchange researchers program, and computer facilities offered by Cecalcula (Venezuela) and CNUSC (France), are gratefully acknowledged.

[1] J. Tyndall, Proc. R. Inst. **6**, 3 (1870).
[2] B. H. Kaye, *Direct Characterization of Fine Particles* (Wiley-Interscience, New York, 1981).
[3] W. F. Phillips, Phys. Fluids **15**, 999 (1972).
[4] L. Talbot, in *Rarefied Gas Dynamics*, edited by S. S. Fisher, Progress in Astronautics and Aeronautics Vol. 74 (AIAA, New York, 1981), Pt. I, p. 487.
[5] B. V. Deryagin and S. P. Bakanov, Dokl. Akad. Nauk. SSSR **117**, 959 (1957) [Sov. Phys. Dokl. **117**, 563 (1957)]; L. Waldmann, Z. Naturforsch. A **14**, 589 (1959); B. V. Deryagin and S. P. Bakanov, Kolloidn Zh. **21**, 377 (1959); S. P. Bakanov and B. V. Derjaguin, Discuss. Faraday Soc. **30**, 130 (1960); L. Waldmann, in *Rarefied Gas Dynamics*, edited by L. Talbot, Advances in Applied Mechanics Series, Suppl. 1 (Academic, New York, 1961), p. 323.
[6] K. Yamamoto, Y. Ishihara, and K. Fujise, J. Phys. Soc. Jpn. **57**, 2386 (1988).
[7] M. M. R. Williams, J. Colloid Interface Sci. **117**, 193 (1987).
[8] J. R. Brock, J. Colloid Interface Sci. **23**, 448 (1967).
[9] P. L. Bhatnagar, E. P. Gross, and M. Krook, Phys. Rev. **94**, 511 (1954).
[10] S. L. Gorelov, Fluid Dyn. **11**, 800 (1977); Y. Sone and K. Aoki, J. Mec. Theor. Appl. **2**, 3 (1983); W. S. Law, Ph.D. thesis, University of Missouri, 1985; S. K. Loyalka, in *Rarefied Gas Dynamics*, edited by V. Boffi and C. Cercignani (Teubner, Stuttgart, 1986), p. 177; K. Yamamoto and Y. Ishihara, Phys. Fluids **31**, 3618 (1988).
[11] Y. Sone and K. Aoki, in *Rarefied Gas Dynamics*, edited by J. L. Potter, Progress in Astronautics and Aeronautics Series (AIAA, New York, 1977), p. 417, and references therein.
[12] M. P. Allen and D. J. Tildesley, *Computer Simulation of Liquids* (Oxford Science Publications, Oxford, 1990), and references therein; *Understanding Molecular Simulation: From Algorithms to Applications*, edited by D. Frenkel and B. Smit (Academic Press, New York, 1996), and references therein.
[13] M. Vergeles, P. Keblinski, J. Koplik, and J. R. Banavar, Phys. Rev. E **53**, 4852 (1996).
[14] J. A. Given and E. Clementi, J. Chem. Phys. **90**, 7376 (1989).
[15] M. Peters, Phys. Rev. E **50**, 4609 (1994).
[16] G. A. Bird, *Molecular Gas Dynamics and the Direct Simulation of Gas Flows* (Oxford University Press, Oxford, 1994); A. L. García, *Numerical Methods for Physics* (Prentice-Hall, Englewood Cliffs, NJ, 1994).
[17] F. J. Alexander, A. L. García, and B. J. Alder, Phys. Rev. Lett. **74**, 5212 (1995).
[18] J. L. Lebowitz and H. Spohn, J. Stat. Phys. **19**, 633 (1978).
[19] A. Tenenbaum, G. Ciccotti, and R. Gallico, Phys. Rev. A **25**, 2778 (1982).
[20] S. Goldstein, J. L. Lebowitz, and E. Presutti (unpublished).
[21] R. Tehver, F. Toigo, J. Koplik, and J. R. Banavar, Phys. Rev. E **57**, R17 (1998).
[22] D.C. Rapaport, *The Art of Molecular Dynamics Simulation* (Cambridge University Press, Cambridge, 1995).
[23] D. M. Gass, J. Chem. Phys. **54**, 1898 (1971).
[24] L. Lees (unpublished).
[25] F. A. Williams, *Combustion Theory* (Addison-Wesley, Reading, MA, 1985).
[26] A. Puhl, M. Malek Mansour, and M. Mareschal, Phys. Rev. E **40**, 1999 (1989).